

Gamma-Ray Shielding Properties of B_4C , Al_2O_3 , Fe_2O_3 , and Their Composites Using MCNP and Phy-X/PSD: A Comparative Study

A. S. Alazouny*, N. I. Abu-Elsaad, and A. M. Reda

Nuclear Physics Department, Faculty of Science, Zagazig University, Zagazig, Egypt

Corresponding author: a.elazouny020@science.zu.edu.eg, amreda26@yahoo.com, nagwa.ibrahim@zu.edu.eg

ABSTRACT: Radiation poses significant hazards across various domains, including environmental, health, and social contexts. As a result, the development of effective shielding materials has become essential in the industry to mitigate these risks. This study focuses on the properties of Boron Carbide (B_4C), Aluminum Oxide (Al_2O_3), and Iron Oxide (Fe_2O_3), all individually and in composite forms with varying weight percentages of each material. The fabricated samples are labeled S1 through S6. The investigation examined key shielding characteristics for gamma rays, including the Mass Attenuation Coefficient (MAC), Linear Attenuation Coefficient (LAC), Half Value Layer (HVL), and Mean Free Path (MFP). These characteristics were analyzed using the Phy-X/PSD software and the results from MCNP (Monte Carlo N-Particle Transport Code). The findings revealed strong agreement between the two calculation methods, with minimal discrepancies when energy reaches above 10 MeV. Among the samples, S2 (Fe_2O_3), S5 (30% B_4C /40% Fe_2O_3 /30% Al_2O_3), demonstrated the best shielding properties, while S1 (B_4C) and S3 (Al_2O_3) exhibited the weakest shielding characteristics by both programs.

KEYWORDS: MCNP, Phys-X/PSD, gamma-ray, attenuation coefficient, mean free path, half value layer, composites.

Date of Submission: 17-02-2025

Date of acceptance: 08-04-2025

I. INTRODUCTION

Gamma rays represent a significant form of nuclear radiation, distinguished by their potent effects and extensive applications across various fields. As the utilization of nuclear radiation continues to expand, the imperative for effective shielding materials becomes increasingly crucial to safeguard both individuals and sensitive equipment from the harmful impacts associated with these high-energy emissions. Therefore, studying Shielding materials showed an enormous development. This development was in many different ways such as studying new single materials or composites. Composite can consist of hundreds of matters in the form of mixed or multi-layer materials. One of the shielding materials is Fe_2O_3 and it is used in life several fields. As well as its high ability in attenuating gamma-rays compared to other different materials [1]. Also, boron carbide (B_4C) which had large investigations on its radiation attenuation ability. B_4C is a particularly important opaque boride ceramic which has high hardness and neutron capturing cross section values; hence, it is utilized as control rods and neutron absorbent material in nuclear reactors. One another common matter which is used in shielding is aluminum oxide (Al_2O_3) [2].

Phy-X/PSD stands for a significant advancement in the field of radiation physics by providing researchers with a powerful, reliable, and easy-to-use platform for the analysis of photon interaction and shielding properties. Its broad application range, coupled with its precision and efficiency, underscores its importance as a tool for advancing research and practical applications in radiation shielding and related fields. On the other hand, Monte Carlo has become instrumental in the simulation of gamma ray interactions due to their ability to accurately model complex physical processes. These stochastic techniques leverage random sampling to solve problems that may be analytically intractable, allowing for precise calculations of gamma ray transport and interaction with matter. By employing Monte Carlo and Phy-X simulations, researchers can gain valuable insights into radiation dosimetry,

medical imaging, and nuclear physics, ultimately enhancing the reliability of predictive models in various scientific and industrial applications.

Researchers seek materials that effectively attenuate nuclear radiation while considering cost, weight, ease of preparation, and environmental impact. Al_2O_3 and Fe_2O_3 are cost-effective and lightweight options, whereas B_4C is light-weight but fragile and highly cost. Therefore, evaluating $\text{B}_4\text{C}/\text{Fe}_2\text{O}_3/\text{Al}_2\text{O}_3$ substituting composites to natural B_4C for radiation shielding become essential, starting with equal proportions and then raise Fe_2O_3 and Al_2O_3 percentages to assess shielding effectiveness while decreasing B_4C . Therefore, in the current work the shielding parameters for single B_4C , Al_2O_3 , and Fe_2O_3 and their composites $\text{B}_4\text{C}/\text{Fe}_2\text{O}_3/\text{Al}_2\text{O}_3$ with a different percentage have been calculated.

II. Materials and Methods

II.1. Sample preparation

Pure powders of B_4C , Al_2O_3 , $\alpha\text{-Fe}_2\text{O}_3$ were used, each material has a purity of 99.98% due to material data sheet from Sigma-Aldrich. The powders were compressed into 6 samples into cylindrical discs with 13 mm diameter and 18 mm height using a vertical pressure mould. These samples are labeled as S1 through S6, as presented in Table (1). The measured densities of all samples were also included in the table.

Table (1): Chemical composition for samples and their densities

Sample	Chemical composition (weight%)			Density
	B_4C	Fe_2O_3	Al_2O_3	
S1	100	-	-	1.7048
S2	-	100%	-	1.7250
S3	-	-	100	1.7024
S4	33.334	33.333	33.333	1.8970
S5	30	40%	30	1.9279
S6	30	30	40	1.9209

II.2. Theoretical basics

II.2.1. Linear attenuation coefficient (μ_t):

Radiation undergoes different interactions with the medium passing through, causing photon attenuation. Assume incident ray intensity (I_0) on material which thickness (x) and the intensity of the passed ray through material (I), by applying The Bear-Lambert law which gives the uncollided photons intensity at the position of detection using narrow beam that incident on shielding material as follows [3]:

$$I = I_0 e^{-\mu_t x} \quad 1$$

where μ_t is the linear attenuation coefficient (LAC) [4].

Then, total LAC can be calculated from the following equation (2):

$$\mu_t = \frac{\ln(I_0/I)}{x} \quad 2$$

II.2.2. Mass attenuation coefficient (μ_t/ρ):

From equation 1, by dividing μ_t by the material density (ρ) in g.cm^{-3} unit the result is (μ_t/ρ), which represents the mass attenuation coefficient (MAC). The total μ_t/ρ of materials with various elements and compounds can be measured from the following equation (3) [3]:

$$\mu_t/\rho = \sum_i w_i (\mu_t/\rho)_i \quad 3$$

where $(\mu_t/\rho)_i$ represents the MAC of element i th and w_i is the relative weight of element i th in the shielding material.

II.2.3. Mean free path (MFP)

The way which a radiation single photon is able to move among two interactions in a row is called MFP or λ which can be determined from the following equation (4) [5]:

$$\lambda = \frac{\int_0^\infty x e^{-\mu_t x} dx}{\int_0^\infty e^{-\mu_t x} dx} = \frac{1}{\mu_t} \quad 4$$

MFP decreases after each collision as it depends on material type and incident radiation energy, MFP has many applications in nuclear shielding [6].

MFP as small value is preferred, as if it is very large, this means that photon will penetrate the assay with no interaction and reach detector without attenuation [6].

II.2.4. Half-value layer (HVL)

The HVL is the substance thickness sufficient to minimize radiation intensity to its half value and it is a good indication for good shielding material and is given by equation (5) [7]:

$$HVL = \ln 2 / \mu_t \quad 5$$

II.3. Monte Carlo and Phy-X simulations

Monte Carlo (MCNP) is usually used to simulate the moving and interactions of photons, neutrons, and electrons. MCNP is a good method to assess the performance of radiation shielding for a substances complex structure. Particles-materials interactions and radiation protection techniques can be measurably analyzed, composition design and substance enhancement can be implemented due to operating standards [8, 9]. Therefore, g researchers used MCNP for their researchers in academic radiation shielding field [10-15].

Many researchers have used Phy-X in their research on the capabilities of material in shielding against nuclear radiations [16-20]. An online software stands on “Photon Shielding and Dosimetry” (PSD) is available at “<https://phy-x.net/PSD>” has been upgraded for shielding and dosimetry computation due to relevant parameters like LAC, MAC ,HVL , MFP, effective atomic number and electron density, and buildup factors. Phy-X has the ability to set up data about shield requirements at significant streak regions of energy from 1 keV to 100 GeV. Some familiar radioactive sources are accessible for users and can choose between them. accordingly, shielding parameters can be measured the for a range of photon energies previously chosen energies. likewise, similar parameter relates to fast neutron removal cross section (FNRCs) be measured for a complex or a substance mix using this system. Phy-X software is accessible for free after registration on the Phy-X platform [16].

III. RESLUTS AND DISCUSSIONS

II.1. Linear and mass attenuation coefficient

The LAC results are illustrated in Figure (1) for the six pure samples, S1, S2, S3, and the three composites S4, S5, and S6 at energies extending start with 0.0015 and end with 10^2 MeV utilizing the Phy-X and MCNP programs. The relative comparison of linear attenuation coefficient results gained from the Phy-X and the MCNP programs demonstrates strong agreement across the studied gamma energy range. Calculations indicate that samples containing Fe_2O_3 (S2, S4, S5, and S6) show evidence of strong gamma-rays attenuation, with S2 having the highest LAC values. Similarly, MCNP calculations confirm that Fe_2O_3 containing samples (S2, S4, S5, and S6) also demonstrate significant attenuation, with S5 showing the highest LAC values.

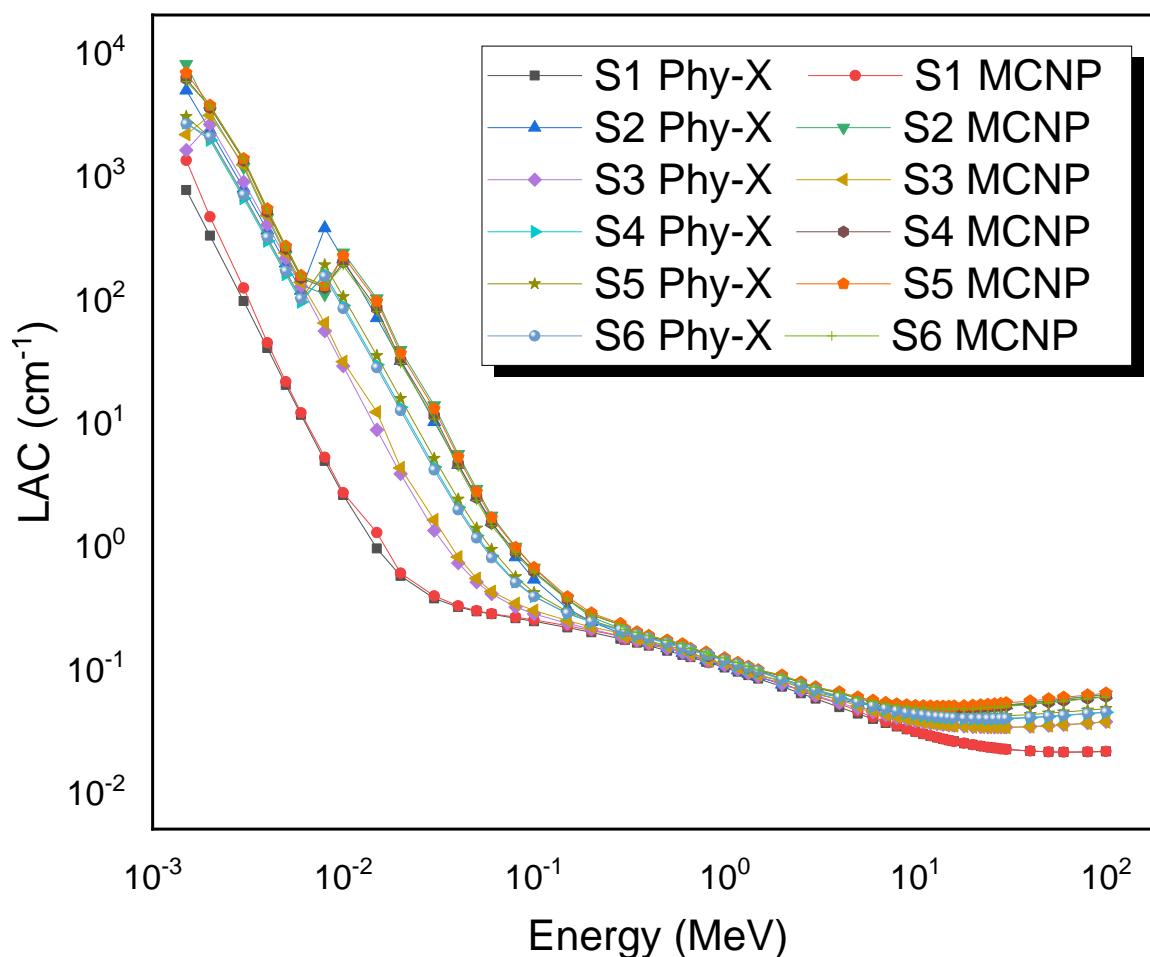


Figure (1): linear attenuation coefficients for samples S1:S6 using MCNP and Phy-X.

Figure (2) shows that the MAC values decrease dramatically while increment of incident radiation energy, up to 10 MeV approximately. Higher than that energy, relative MAC constancy can be noticed while the incident energy of the photons is getting to increase with little increment. This attitude indicates the 3 most important interactions among the shield substance and radiation: photoelectric effect, Compton effect, and pair production respectively. As usual, it was observed that the superior MAC values appear for low energy photons because of the increment of the cross section of scattering interaction of the photoelectric effect, that is concerns with $E^{3.5}$ and $Z^{4.5}$ [21]. The MAC measured peak close to 0.0015 MeV photon energy is recognized as the K-absorption of Al ($Z=13$) existing in sample S3. Moreover, the peaks near the 0.008 MeV energy refers to the K-absorption of Fe ($Z=26$) existing in the samples S2, S5, S4, and S6 contents. Then, MAC values change slowly with little increment with photon energy region in which Compton interaction cross section is the dominance, because it varies with E^{-1} and Z [21]. Also, the figures show that the MAC values for all samples are close due to investigation. At higher energies, from 20MeV, MAC values have sluggish increment because of the pair production interaction cross-section dominance. It changes in this energy region with $\log(E)$ and Z^2 [21]. The results of the MAC by the two programs consistent that samples containing Fe_2O_3 (S2, S4, S5, and S6 respectively) show superior capability in attenuating gamma-rays versus the other samples, especially composite S5 have the highest MAC values.

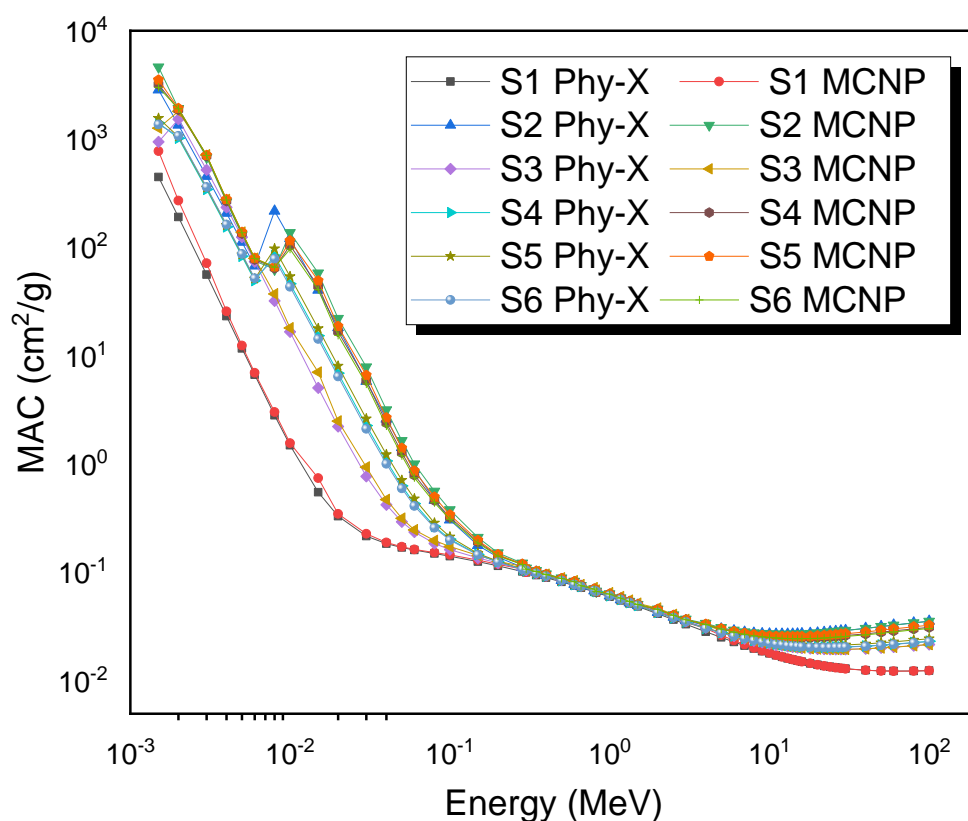


Figure (2): Mass attenuation coefficient for samples S1:S6 using MCNP and Phy-X.

III.2. Mean free path and Half value layer

MFP and HVL for gamma-rays shielding substances using Phy-X program are automatically calculated with the program, but MCNP only gives the MAC values then HVL and MFP can be calculated from equations (4) and (5). The MFP and HVL results are illustrated in Figures 3 and 4. The figures show an instant increment in their values while increasing photon energy for the 6 samples investigated. The curves of MFP and HVL values illustrate the impact of various interaction mechanisms among γ -rays and samples. At higher γ -ray energies, MFP measurements extend from 20 to 47 cm, while HVL values extend from 14 to 33 cm for the samples studied. At intermediate γ -ray energies, Compton interaction influences the MFP and HVL measurements, showing minimal differences among the materials examined. In the weak energy scale, the photoelectric phenomenon becomes prominent, causing both MFP and HVL values to decrease as γ -ray energy declines. This indicates that as the photoelectric effect dominates lower energies, γ -rays have a short mean distance before absorption. The samples (S2 and S5) that contain Fe_2O_3 show the best MFP and HVL results than the rest, as it has the lowest results among them. The divergent of the HVL measurements to the incident photon energies demonstrate MFP same nature, so the two parameters are mainly dependent on the LAC measurements with some variance with the equation constant.

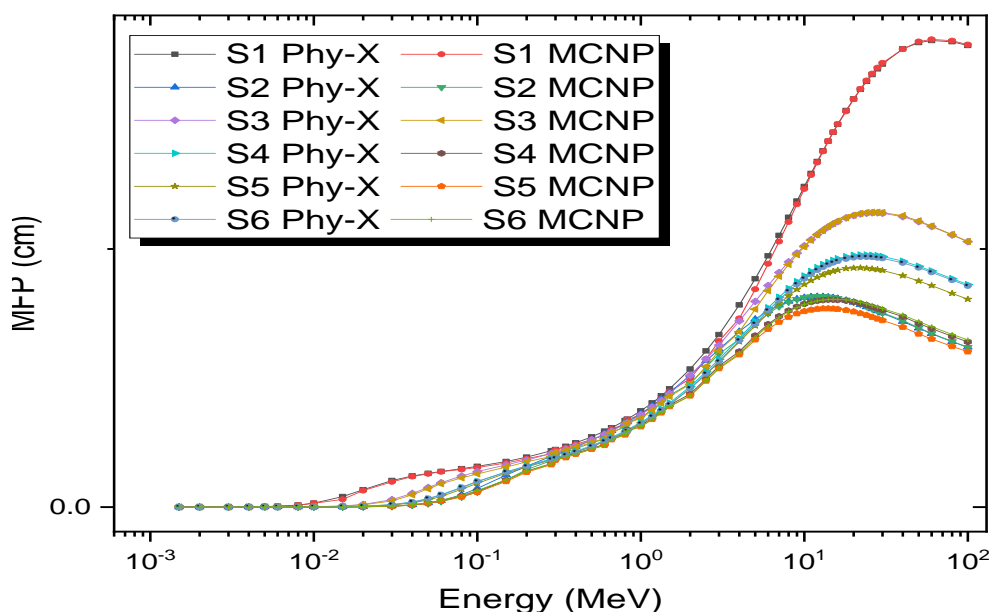


Figure (3): MFP for samples S1:S6 using MCNP and Phy-X.

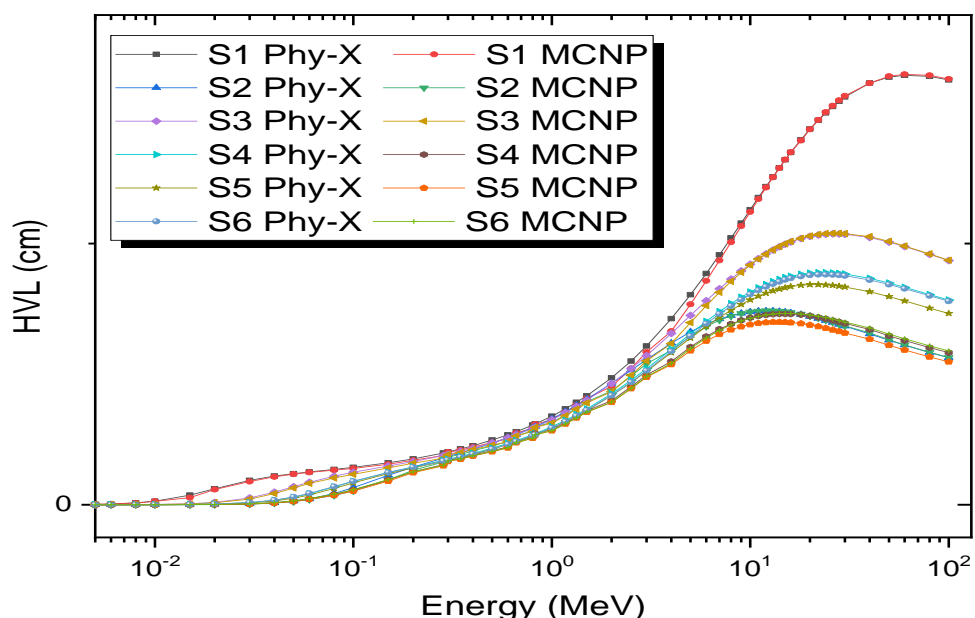


Figure (4): HVL for samples S1:S6 using MCNP and Phy-X.

IV. Conclusion

In this investigation, the six samples using Phy-X and MCNP indicate that the presence of Fe_2O_3 improves the material efficacy for shielding against gamma-rays. Results show that S2, S4, S5 and S6 have the best gamma-ray attenuation compared to other samples. On the contrary S1 and S3 showed the least shielding capability. The results show good agreement between Phy-X and MCNP calculations. The consistency between Phy-X and MCNP confirms the reliability and accuracy of the computed attenuation values. This validation highlights the robustness of both approaches in modeling gamma-ray interactions with materials, reinforcing the credibility of the obtained results for radiation shielding and material analysis applications.

REFERENCES

1. Reda, A., W. Kansouh, and E.J.P.S. Eid, *Effect of $\text{Fe}_2\text{O}_3/\text{Al}$ addition on the neutron*

- shielding, microstructure, thermal, and mechanical properties of HDPE composites. 2022. **97**(6): p. 065301.
2. Fu, S., et al., *Synthesis and characterization of a high-strength alumina ceramic reinforced by AlN-Al₂O₃ coating*. Journal of Materials Science, 2024. **59**(31): p. 14235-14244.
 3. Reda, A. and A.J.P.i.N.E. El-Daly, *Gamma ray shielding characteristics of Sn-20Bi and Sn-20Bi-0.4 Cu lead-free alloys*. 2020. **123**: p. 103304.
 4. ABDLHAMED, A.F.A., *GRADUATE SCHOOL OF NATURAL AND APPLIED SCIENCES*. 2018, SÜLEYMAN DEMİREL UNIVERSITY.
 5. Tsoulfanidis, N. and S. Landsberger, *Measurement & detection of radiation*. 2021: CRC press.
 6. Rinard, P.J.P.n.a.o.n.m., *Neutron interactions with matter*. 1991(375-377).
 7. Aygun, B., *Neutron and gamma radiation shielding Ni based new type super alloys development and production by Monte Carlo Simulation technique*. Radiation Physics and Chemistry, 2021. **188**.
 8. Liu, Y.S., et al., *Gamma radiation shielding property of continuous fiber reinforced epoxy matrix composite containing functional filler using Monte Carlo simulation*. Nuclear Materials and Energy, 2022. **33**.
 9. Harrison, R.L. *Introduction to monte carlo simulation*. in *AIP conference proceedings*. 2010. NIH Public Access.
 10. Reda, A., A. Azab, and G.J.P.S. Turkey, *Gamma-ray shielding, electrical, and magnetic properties of α -Fe₂O₃/Al/HDPE nanocomposites*. 2022. **97**(9): p. 095303.
 11. Issa, S.A., et al., *Effect of Bi₂O₃ content on mechanical and nuclear radiation shielding properties of Bi₂O₃-MoO₃-B₂O₃-SiO₂-Na₂O-Fe₂O₃ glass system*. 2019. **13**: p. 102165.
 12. Akçalı, Ö., et al., *An investigation on gamma-ray shielding properties of quaternary glassy composite (Na₂Si₃O₇/Bi₂O₃/B₂O₃/Sb₂O₃) by BXCOP and MCNP 6.2 code*. 2020. **125**: p. 103364.
 13. Alothman, M.A., et al., *The significant role of CeO₂ content on the radiation shielding performance of Fe₂O₃-P₂O₅ glass-ceramics: Geant4 simulations study*. 2021. **96**(11): p. 115305.
 14. Issa, S.A. and H.J.C.I. Tekin, *The multiple characterization of gamma, neutron and proton shielding performances of xPbO-(99-x) B₂O₃-Sm₂O₃ glass system*. 2019. **45**(17): p. 23561-23571.
 15. Toker, O., et al., *Evaluation of three different glassy composites (quinary matrix designed using Cr₂O₃/Na₂O/MnO₂) in respect of radiation shielding behaviors*. 2021. **176**(9-10): p. 967-981.
 16. Şakar, E., et al., *Phy-X/PSD: development of a user friendly online software for calculation of parameters relevant to radiation shielding and dosimetry*. 2020. **166**: p. 108496.
 17. Al-Hadeethi, Y. and M.I. Sayyed, *Evaluation of gamma ray shielding characteristics of CaF₂-BaO -P₂O₅ glass system using Phy-X / PSD computer program*. Progress in Nuclear Energy, 2020. **126**: p. 103397.
 18. An, J.M., et al., *Evaluation of gamma and neutron shielding capacities of tellurite glass system with Phy-X simulation software*. Physica B: Condensed Matter, 2022. **634**: p. 413433.
 19. Gunoglu, K., H. Varol Özkavak, and İ. Akkurt, *Evaluation of gamma ray attenuation properties of boron carbide (B₄C) doped AISI 316 stainless steel: Experimental, XCOM and Phy-X/PSD database software*. Materials Today Communications, 2021. **29**: p. 102793.
 20. Günoğlu, K. and İ.J.I. AKKURT, *Gamma-ray attenuation properties carbide compounds (WC, Mo₂C, TiC, SiC, B₄C) using Phy-X/PSD software*. 2024. **1**(1): p. 1-8.
 21. Wood, J., *Computational methods in reactor shielding*. 2013: Elsevier.